

Cyanide-Bridged Iron–Copper Molecular Squares with Doublet and Quintet Spin Ground States

Hiroki Oshio,^{*,†} Osamu Tamada,[†] Hironori Onodera,[†] Tasuku Ito,[†] Tadaaki Ikoma,[‡] and Shozo Tero-Kubota[‡]

Department of Chemistry, Graduate School of Science, Tohoku University, Aoba-ku, Sendai 980-8578, Japan, and Institute for Chemical Reaction Science, Tohoku University, Aoba-ku Sendai 980-8578, Japan

Received May 26, 1999

Reactions of $[\text{Fe}^{\text{II}}(\text{CN})_2(\text{bpy})_2]$ and $[\text{Fe}^{\text{III}}(\text{CN})_2(\text{bpy})_2](\text{PF}_6)$ with $[\text{Cu}^{\text{II}}(\text{bpy})(\text{CH}_3\text{OH})_2](\text{PF}_6)_2$ in methanol yielded cyanide-bridged cyclic tetranuclear complexes of $[\text{Fe}^{\text{II}}\text{Cu}^{\text{II}}_2(\mu\text{-CN})_4(\text{bpy})_6](\text{PF}_6)_4 \cdot 2\text{H}_2\text{O} \cdot 4\text{CHCl}_3$ (**1**) and $[\text{Fe}^{\text{III}}\text{Cu}^{\text{II}}_2(\mu\text{-CN})_4(\text{bpy})_6](\text{PF}_6)_6 \cdot 4\text{CH}_3\text{CN} \cdot 2\text{CHCl}_3$ (**2**), respectively. In the squares of **1** and **2**, the $\text{Fe}^{2+/3+}$ (low-spin) and Cu^{2+} ions are alternately bridged by the cyanide ions, the carbon atoms of which coordinate to the iron ions. Variable-temperature magnetic susceptibility studies of complexes revealed that the Cu^{2+} ions in **1** are magnetically isolated. In the square of **2**, the adjacent Fe^{3+} and Cu^{2+} ions were ferromagnetically coupled through the cyanide bridges with a J_1 value of $+6.3(1) \text{ cm}^{-1}$ and the weaker antiferromagnetic interactions between the orthogonal $\text{Fe}^{3+} \cdots \text{Fe}^{3+}$ and $\text{Cu}^{2+} \cdots \text{Cu}^{2+}$ pairs are operative ($J_2 = -3.1(1) \text{ cm}^{-1}$). The propagation of the ferromagnetic interaction in **2** can be understood by the orthogonal magnetic orbitals of the low-spin Fe^{3+} ($d\pi$) and Cu^{2+} ($d\sigma$) ions. Cyclic voltammograms of the squares have been recorded and discussed. Crystal data for **1**: triclinic space group $P\bar{1}$, $a = 14.491(4) \text{ \AA}$, $b = 15.312(4) \text{ \AA}$, $c = 12.959(3) \text{ \AA}$, $\alpha = 91.38(2)^\circ$, $\beta = 109.56(2)^\circ$, $\gamma = 65.41(2)^\circ$, $Z = 1$. Crystal data for **2**: triclinic space group $P\bar{1}$, $a = 14.472(9) \text{ \AA}$, $b = 15.310(6) \text{ \AA}$, $c = 12.523(5) \text{ \AA}$, $\alpha = 102.58(3)^\circ$, $\beta = 107.19(4)^\circ$, $\gamma = 75.08(4)^\circ$, $Z = 1$.

Introduction

Self-assembly by means of coordination bonds has been applied to construct functional nanoscaled supramolecules.¹ In the assembled systems not only are reaction sites available but also specific electronic states due to metal–metal interactions play an important role in their functions. A cyclic tetranuclear system, called a molecular square, is one of the simplest models of the infinite assembly, and it can be used to study interactions between metal centers. A variety of methodologies have been proposed and used to prepare molecular squares. Polypyridyl bridging ligands were used to synthesize squares and even grid compounds.² Square planar coordination geometry of platinum(II) and palladium(II) ions has been reported to give facile formation of the squares, and this strategy was employed to the more extended systems.³ On the other hand, cyanide-bridged infinite systems called Prussian blue analogues⁴ and high-spin

clusters⁵ have attracted intense research interest from the magnetic viewpoints of high- T_c and light-induced magnets. Although cyanide ions have the potential to bridge a variety of metal ions and form cluster compounds, a cyanide-bridged high-spin square has not been prepared. We report herein cyanide-bridged iron(II)–copper(II) and iron(III)–copper(II) molecular squares with doublet and quintet spin ground states, respectively.

Experimental Section

Syntheses. Chemicals were obtained from standard sources and were used as received.

$[\text{Fe}^{\text{II}}\text{Cu}^{\text{II}}_2(\mu\text{-CN})_4(\text{bpy})_6](\text{PF}_6)_4 \cdot 2\text{H}_2\text{O} \cdot 4\text{CHCl}_3$ (**1**). $[\text{Fe}^{\text{II}}(\text{CN})_2(\text{bpy})_2]$ ⁶ (55 mg, 0.13 mmol) in MeOH (25 mL) was added to a solution of $[\text{Cu}^{\text{II}}(\text{bpy})(\text{CH}_3\text{OH})_2](\text{NO}_3)_2 \cdot 3\text{H}_2\text{O}$ (50 mg, 0.13 mmol) in methanol

[†] Department of Chemistry, Graduate School of Science.

[‡] Institute for Chemical Reaction Science.

- (1) (a) Lehn, J.-M. *Supramolecular Chemistry—Concepts and Perspectives*; VCH: Weinheim, 1995. (b) Balzani, V.; Scandola, F. *Supramolecular Photochemistry*; Horwood: Chichester, U.K., 1991; Chapters 5 and 6.
- (2) (a) Bassani, D. M.; Lehn, J.-M.; Fromm, K.; Frenske, D. *Angew. Chem., Int. Ed.* **1998**, *37*, 2364. (b) Hanan, G. S.; Volkmer, D.; Schubert, U. S.; Lahn, J.-M.; Baum, G.; Frenske, D. *Angew. Chem., Int. Ed. Engl.* **1997**, *36*, 1842. (c) Drain, C. M.; Lehn, J.-M. *J. Chem. Soc., Chem. Commun.* **1994**, 2313. (d) Weissbuch, I.; Baxter, P. N. W.; Cohen, S.; Cohen, H.; Kjaer, K.; Howes, P. B.; Als-Nielsen, J.; Hanan, G. S.; Schubert, U. S.; Lehn, J.-M.; Leiserowitz, L.; Lahav, M. *J. Am. Chem. Soc.* **1998**, *120*, 4850. (e) Slone, R. V.; Yoon, D. L.; Calhoun, R. M.; Hupp, J. Y. *J. Am. Chem. Soc.* **1995**, *117*, 11813. (f) Slone, R. V.; Hupp, J. T.; Stern, C. L.; Albrecht-Schmitt, T. E. *Inorg. Chem.* **1996**, *35*, 4096. (g) Klausmeyer, K. K.; Rauchfuss, T. B.; Willson, S. R. *Angew. Chem., Int. Ed.* **1998**, *37*, 1694.

- (3) (a) Manna, J.; Kuehl, C. J.; Whiteford, J. A.; Stang, P. J.; Muddiman, D. C.; Hofstadler, S. A.; Smith, R. D. *J. Am. Chem. Soc.* **1997**, *119*, 11611. (b) Stang, P. J.; Cao, D. H.; Chen, K.; Gray, G. M.; Muddiman, D. C.; Smith, R. D. *J. Am. Chem. Soc.* **1997**, *119*, 5163. (c) Slone, R. V.; Yoon, D. L.; Calhoun, R. M.; Hupp, J. T. *J. Am. Chem. Soc.* **1995**, *117*, 11813. (d) Stang, P. J.; Persky, N. E.; Manna, J. *J. Am. Chem. Soc.* **1997**, *119*, 4777. (e) Stang, P. J. *Chem.—Eur. J.* **1998**, *4*, 19. (f) Fujita, M.; Oguro, D.; Miyazawa, M.; Oka, H.; Yamaguchi, K.; Ogura, K. *Nature* **1995**, *378*, 469.
- (4) (a) Ferlay, S.; Mallah, T.; Ouahès, R.; Veillet, P.; Verdager, M. *Nature* **1995**, *378*, 701. (b) Entley, W. R.; Girolami, G. S. *Science* **1995**, *268*, 397. (c) Sato, O.; Iyoda, T.; Fujishima, A.; Hashimoto, K. *Science* **1996**, *271*, 49. (d) Larionova, J.; Clérac, R.; Sanchiz, J.; Kahn, O.; Golhen, S.; Quahab, L. *J. Am. Chem. Soc.* **1998**, *120*, 13088.
- (5) (a) Henrich, J. L.; Berseth, P. A.; Long, J. R. *Chem. Commun.* **1998**, 1231. (b) Scuiller, A.; Mallah, T.; Verdager, M.; Nivorozhkin, A.; Tholence, J.-L.; Veillet, P. *New J. Chem.* **1996**, *20*, 1. (c) Vernier, N.; Bellessa, G.; Mallah, T.; Verdager, M. *Phys. Rev. B* **1997**, *56*, 75. (d) Klausmeyer, K. K.; Rauchfuss, T. B.; Willson, S. R. *Angew. Chem., Int. Ed.* **1998**, *37*.
- (6) Shilt, A. A. *Inorg. Synth.* **1970**, *12*, 248.
- (7) Jaeger, F. M.; Dijk, J. A. Z. *Anorg. Chem.* **1936**, *227*, 273.

Table 1. Crystallographic Data for $[\text{Fe}_2\text{Cu}_2(\mu\text{-CN})_4(\text{bpy})_6](\text{PF}_6)_4 \cdot 2\text{H}_2\text{O} \cdot 4\text{CHCl}_3$ (**1**) and $[\text{Fe}_2\text{Cu}_2(\mu\text{-CN})_4(\text{bpy})_6](\text{PF}_6)_6 \cdot 4\text{CH}_3\text{CN} \cdot 2\text{CHCl}_3$ (**2**)

	1	2
empirical formula	$\text{C}_{65}\text{H}_{48}\text{Cl}_3\text{Cu}_2\text{F}_{24}\text{Fe}_2\text{N}_{16}\text{O}_2\text{P}_4$	$\text{C}_{70}\text{H}_{66}\text{Cl}_6\text{Cu}_2\text{F}_{36}\text{Fe}_2\text{N}_{20}\text{P}_6$
fw	2010.20	2508.73
space group	$P\bar{1}$	$P\bar{1}$
a , Å	14.491(4)	14.472(9)
b , Å	15.312(4)	15.310(6)
c , Å	12.959(3)	12.523(5)
α , deg	91.38(2)	102.58(3)
β , deg	109.56(2)	107.19(4)
γ , deg	65.41(2)	75.08(4)
V , Å ³	2441.3(12)	2531(2)
Z	1	1
ρ (calcd), g cm ⁻³	1.367	1.646
T , °C	-60	-60
λ , Å	0.710 73	0.710 73
μ , mm ⁻¹	0.959	1.065
transm coeff	0.911–0.977	0.950–0.998
$R1^a$	0.0857	0.0541
$wR2^b$	0.2296	0.1368

^a $R1 = \sum ||F_o| - |F_c|| / \sum |F_o|$. ^b $wR2 = [\sum [w(F_o^2 - F_c^2)^2] / \sum [w(F_o^2)^2]]^{0.5}$; calcd for **1**, $w = 1/[\sigma^2(F_o^2) + (0.1590P)^2 + 5.9442P]$, calcd for **2**, $w = 1/[\sigma^2(F_o^2) + (0.0847P)^2 + 2.2356P]$ where $P = (F_o^2 + 2F_c^2)/3$.

(25 mL). After 3 days of stirring, the addition of NH_4PF_6 (62 mg, 0.38 mmol) in methanol (25 mL) gave a deep red powder. Recrystallization by slow diffusion of chloroform into an acetonitrile solution yielded dark red crystals of **1**.

$[\text{Fe}^{\text{III}}_2\text{Cu}^{\text{II}}_2(\mu\text{-CN})_4(\text{bpy})_6](\text{PF}_6)_6 \cdot 4\text{CH}_3\text{CN} \cdot 2\text{CHCl}_3$ (**2**). $[\text{Fe}^{\text{III}}(\text{CN})_2(\text{bpy})_2](\text{PF}_6)_8$ (61 mg, 0.13 mmol) in MeOH (25 mL) was added to a solution of $[\text{Cu}^{\text{II}}(\text{bpy})(\text{CH}_3\text{OH})_2](\text{NO}_3)_2 \cdot 3\text{H}_2\text{O}$ (50 mg, 0.13 mmol) in methanol (25 mL). After 3 days of stirring, the addition of NH_4PF_6 (62 mg, 0.38 mmol) in methanol (25 mL) gave a brown powder. Recrystallization by slow diffusion of chloroform into an acetonitrile solution yielded dark brown crystals of **2**.

Crystallographic Data Collection and Structure Determination. A dark red tablet ($0.6 \times 0.5 \times 0.3$ mm³) of **1** and a dark brown tablet ($0.3 \times 0.2 \times 0.06$ mm³) of **2** were mounted at the ends of glass fibers, respectively. Intensity data were collected at -60 °C on Rigaku AFC7S diffractometer equipped with graphite-monochromated Mo K α radiation, employing ω - 2θ scan techniques. Unit cell parameters were obtained by least-squares refinements of 20 reflections ($25^\circ < 2\theta < 30^\circ$). Totals of 11 365 and 12 083 reflections ($2^\circ < \theta < 27.5^\circ$) were respectively collected for **1** and **2**, which yield 10 936 ($R_{\text{int}} = 0.0406$) and 11 622 ($R_{\text{int}} = 0.0136$) independent reflections, 6322 and 7895 of them with $I > 2\sigma(I)$ for **1** and **2**, respectively. The diffraction data were corrected for Lorentz and polarization effects, and absorption corrections were made by the analytical method, which gave relative transmissions of 0.911–0.977 and 0.950–0.998 for **1** and **2**, respectively. Crystallographic data are given in Table 1. The structures were solved by the conventional heavy atom method and subsequent Fourier syntheses; anisotropic full-matrix least-squares refinements on F^2 were done by using SHELX-93 (G. M. Sheldrick, University of Göttingen, 1993), where hydrogen atoms were included in calculated positions and refined with isotropic thermal parameters riding on those of the parent atoms. One of the PF_6^- anions in **1** was found to be disordered around the F–P–F axis, and a split-atom model with a 1:1 occupancy was applied.

Magnetic and IR Measurements. Magnetic susceptibility data in the temperature range 2.0–300 K were collected with an applied 10 kG field with the use of a Quantum Design model MPMS SQUID magnetometer. Pascal's constants⁹ were used to determine the constituent atom diamagnetism. IR spectra was obtained by using a JASCO FT/IR-630 IR spectrometer.

Electrochemical Measurements. Cyclic voltammetry (CV) was carried out in nitrogen-purged acetonitrile solution at room temperature with the use of a BAS CV-50W voltammetric analyzer. A glassy carbon

electrode was used as the working electrode. The counter electrode was a platinum coil, and the reference electrode was a saturated sodium calomel electrode (SSCE). The concentration of the complexes was 1×10^{-3} M, and tetrabutylammonium hexafluorophosphate (0.1 M) was used as the supporting electrolyte. CV was performed at a scan rate of 100 mVs⁻¹. All of the half-wave potentials $E_{1/2} = (E_{\text{pc}} + E_{\text{pa}})/2$, where E_{pc} and E_{pa} are the cathodic and anodic peak potential, respectively, are reported with respect to the SSCE.

Results and Discussion

Structures of $[\text{Fe}^{\text{II}}_2\text{Cu}^{\text{II}}_2(\mu\text{-CN})_4(\text{bpy})_6](\text{PF}_6)_4 \cdot 2\text{H}_2\text{O} \cdot 4\text{CHCl}_3$ (1**) and $[\text{Fe}^{\text{III}}_2\text{Cu}^{\text{II}}_2(\mu\text{-CN})_4(\text{bpy})_6](\text{PF}_6)_6 \cdot 4\text{CH}_3\text{CN} \cdot 2\text{CHCl}_3$ (**2**).** The structures of the cations **1** and **2** are depicted in Figure 1, and Tables 2 and 3 summarize selected bond distances and angles. Complex cations **1** and **2** having an inversion center in the molecule are tetranuclear macrocycles with the overall geometry being nearly square, in which low-spin Fe^{2+} or Fe^{3+} and Cu^{2+} ions are alternately bridged by cyanide ions. The orientation of the cyanide groups is, however, ambiguous, and they might be disordered. Cyanide carbon and nitrogen atoms act as π -acceptor and σ -donor, respectively, and the iron ion regarded as a π -donor prefers being coordinated by the cyanide carbon atoms. X-ray structure analyses of a cyanide-bridged iron square, $[\text{Fe}^{\text{II}}_4(\mu\text{-CN})_4(\text{bpy})_8](\text{PF}_6)_4 \cdot 4\text{H}_2\text{O}$,¹⁰ revealed that the bond distances of Fe^{2+} -C (cyanide carbon) and Fe^{2+} -N (cyanide nitrogen) are in the ranges 1.899(4)–1.927(4) Å and 1.929(4)–1.950(4) Å, respectively. The observed Fe^{2+} -C bond distances (1.882(7) and 1.886(6) Å) in **1** are shorter than the corresponding bond distances in $[\text{Fe}^{\text{II}}_4(\mu\text{-CN})_4(\text{bpy})_8](\text{PF}_6)_4 \cdot 4\text{H}_2\text{O}$, and the coordination of the cyanide nitrogen atom to the Fe^{2+} ion is expected to cause an Fe^{2+} -N bond length longer than 1.9 Å. On the other hand, the Fe^{3+} -C bond lengths in a mononuclear complex, $[\text{Fe}^{\text{III}}(\text{CN})_2(\text{bpy})_2](\text{ClO}_4)$,¹¹ are reported to be 1.931(7) and 1.928(7) Å, which is in good agreement with the bond length of the Fe^{3+} -C bonds (1.930(4)–1.931(4) Å) in **2**. Therefore, we concluded that the cyanide carbon atoms coordinate to the iron ions in **1** and **2**. It should be noted that the observed small isotropic displacement parameters for the cyanide carbon and nitrogen atoms (less than 40×10^{-3} Å² for

(8) Shilt, A. A. *J. Am. Chem. Soc.* **1960**, *82*, 3000.

(9) Hatfield, W. E. In *Theory and Application of Molecular Paramagnetism*; Boudreaux, E. A., Mulay, L. N., Eds.; Wiley and Sons: New York, 1976; pp 491–495.

(10) X-ray structure data for $[\text{Fe}^{\text{II}}_4(\mu\text{-CN})_4(\text{bpy})_8](\text{PF}_6)_4 \cdot 4\text{H}_2\text{O}$ will be submitted.

(11) (a) Lu, T.-H.; Kao, H.-Y.; Wu, D. I.; Kong, K. C.; Cheng, C. H. *Acta Crystallogr.* **1988**, *C44*, 1184. (b) Shilt, A. A. *Inorg. Chem.* **1964**, *3*, 1323.

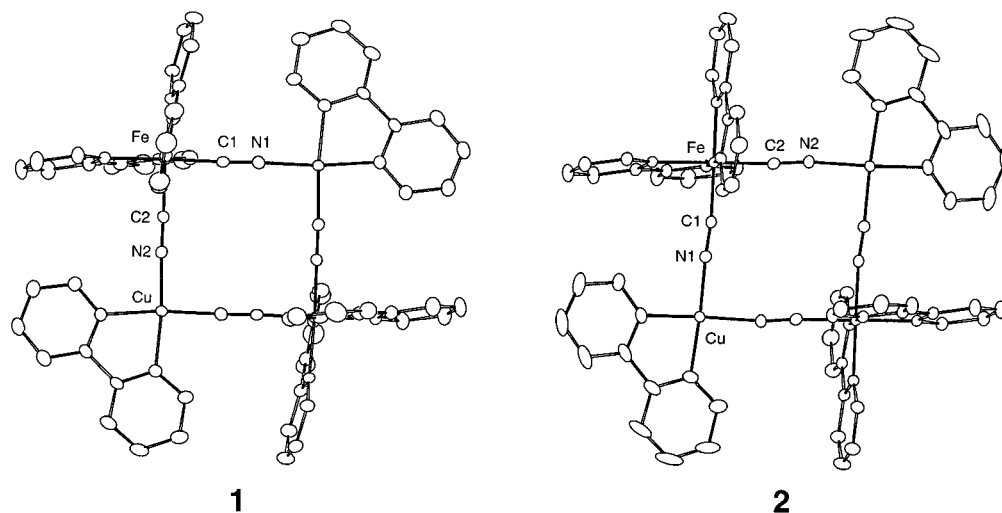


Figure 1. ORTEP diagrams of $[\text{Fe}_2\text{Cu}_2(\mu\text{-CN})_4(\text{bpy})_6]^{4+}$ (**1**) and $[\text{Fe}_2\text{Cu}_2(\mu\text{-CN})_4(\text{bpy})_6]^{6+}$ (**2**).

Table 2. Selected Bond Lengths (Å) Angles (deg) for $[\text{Fe}_2\text{Cu}_2(\mu\text{-CN})_4(\text{bpy})_6](\text{PF}_6)_4 \cdot 2\text{H}_2\text{O} \cdot 4\text{CHCl}_3$ (**1**)

Cu–N(2)	1.935(6)	Cu–N(1)	1.945(6)
Cu–N(8)	2.003(6)	Cu–N(7)	2.010(5)
Fe–C(1)	1.882(7)	Fe–C(2)#1 ^a	1.886(6)
Fe–N(5)	1.977(6)	Fe–N(3)	1.978(6)
Fe–N(4)	1.991(5)	Fe–N(6)	1.996(5)
N(1)–C(1)	1.157(8)	N(2)–C(2)	1.154(8)
Cu–O(1)	2.64(2)		
N(2)–Cu–N(1)	92.7(2)	N(2)–Cu–N(8)	93.2(2)
N(1)–Cu–N(8)	173.6(2)	N(2)–Cu–N(7)	170.5(2)
N(1)–Cu–N(7)	93.7(2)	N(8)–Cu–N(7)	80.7(2)
N(2)–Cu–O(1)	89.3(6)	N(1)–Cu–O(1)	86.5(5)
N(8)–Cu–O(1)	91.2(5)	N(7)–Cu–O(1)	98.1(6)
C(1)–Fe–C(2)#1	89.3(3)	C(1)–Fe–N(5)	90.4(3)
C(2)#1–Fe–N(5)	94.1(3)	C(1)–Fe–N(3)	94.6(3)
C(2)#1–Fe–N(3)	89.2(3)	N(5)–Fe–N(3)	174.1(2)
C(1)–Fe–N(4)	175.0(3)	C(2)#1–Fe–N(4)	88.9(2)
N(5)–Fe–N(4)	94.4(2)	N(3)–Fe–N(4)	80.7(2)
C(1)–Fe–N(6)	87.5(2)	C(2)#1–Fe–N(6)	174.2(3)
N(5)–Fe–N(6)	81.1(2)	N(3)–Fe–N(6)	95.8(2)
N(4)–Fe–N(6)	94.7(2)	C(1)–N(1)–Cu	177.5(6)
C(2)–N(2)–Cu	173.6(6)	N(1)–C(1)–Fe	178.1(6)
N(2)–C(2)–Fe#1	178.8(6)		

^a Symmetry transformations used to generate equivalent atoms: (#1) $-x + 1, -y, -z + 2$.

both atoms) in **1** and **2** exclude the possibility of positional disorder of the carbon and nitrogen atoms. The bond angles of C–Fe–C and N–Cu–N for **1** are 89.3(3)° and 92.7(2)°, and those for **2** are 91.8(2)° and 88.5(1)°, respectively. The edge to edge distances (Fe···Cu) are 4.983(2) and 4.970(2) Å for **1** and 5.037(2) and 5.046(3) Å for **2**. The size of the square **1** is slightly smaller than that of **2**. The coordination geometry of Cu²⁺ ions in **1** and **2** can be regarded as square planar with coordination of bpy and cyanide groups, and solvent molecules weakly coordinated at the fifth position. The Cu–N bond distances are in the range 1.935(6)–2.010(5) Å, and the magnetic orbitals of the Cu²⁺ ions are the $d_{x^2-y^2}$ orbitals which direct at the coordinated cyanide groups. Six coordination sites of the iron ions in **1** and **2** are occupied by the four nitrogen atoms from bpy and two of the cyanide carbon atoms. The Fe²⁺–C bond distances (1.882(7) and 1.886(6) Å) in **1** are slightly shorter than the Fe³⁺–C bond lengths of **2** (1.930(4)–1.931(4) Å), which is due to the more pronounced π -back-donation in the low-spin Fe²⁺ ions. The C–N bond distances and CN stretching frequency of the cyanide in **1** and **2** are not so sensitive to the

Table 3. Selected Bond Lengths (Å) and Angles (deg) for $[\text{Fe}_2\text{Cu}_2(\mu\text{-CN})_4(\text{bpy})_6](\text{PF}_6)_6 \cdot 4\text{CH}_3\text{CN} \cdot 2\text{CHCl}_3$ (**2**)

Cu–N(1)	1.970(3)	Cu–N(2)#1 ^a	1.981(3)
Cu–N(8)	1.991(3)	Cu–N(7)	1.997(3)
Cu–N(9)	2.298(4)	N(2)–Cu#1	1.981(3)
Fe–C(1)	1.931(4)	Fe–C(2)	1.930(4)
Fe–N(3)	1.981(3)	Fe–N(5)	1.970(3)
Fe–N(4)	1.968(3)	Fe–N(6)	1.965(3)
N(1)–C(1)	1.142(5)	N(2)–C(2)	1.142(5)
N(1)–Cu–N(2)#1	88.52(13)	N(1)–Cu–N(8)	175.69(14)
N(2)#1–Cu–N(8)	94.88(14)	N(1)–Cu–N(7)	94.64(14)
N(2)#1–Cu–N(7)	163.10(13)	N(8)–Cu–N(7)	81.3(2)
N(1)–Cu–N(9)	94.7(2)	N(2)#1–Cu–N(9)	94.9(2)
N(8)–Cu–N(9)	87.7(2)	N(7)–Cu–N(9)	101.3(2)
C(1)–N(1)–Cu	176.3(3)	C(2)–N(2)–Cu#1	171.9(3)
N(1)–C(1)–Fe	173.5(3)	N(2)–C(2)–Fe	175.5(3)
C(1)–Fe–C(2)	91.8(2)	C(1)–Fe–N(6)	176.62(13)
C(2)–Fe–N(6)	88.77(14)	C(1)–Fe–N(4)	85.87(14)
C(2)–Fe–N(4)	95.78(14)	N(6)–Fe–N(4)	97.40(12)
C(1)–Fe–N(5)	94.71(14)	C(2)–Fe–N(5)	84.87(14)
N(6)–Fe–N(5)	82.00(13)	N(4)–Fe–N(5)	179.12(12)
C(1)–Fe–N(3)	87.64(14)	C(2)–Fe–N(3)	177.62(13)
N(6)–Fe–N(3)	91.97(12)	N(4)–Fe–N(3)	81.88(13)
N(5)–Fe–N(3)	97.48(13)		

^a Symmetry transformations used to generate equivalent atoms: #1– $x + 1, -y + 1, -z + 1$.

oxidation state of iron ions, which are in contrast to mononuclear complexes. The C–N(cyanide) bond lengths in $[\text{Fe}(\text{CN})_2(\text{phen})_2]^{12}$ and $[\text{Fe}(\text{CN})_2(\text{bpy})_2](\text{ClO}_4)^{11a}$ are 1.149(7)–1.151(7) Å and 1.123(9)–1.135(1) Å, respectively, while the former showed strong IR signals of $\nu(\text{CN})$ at 2075 and 2062 cm^{-1} and the latter has a barely detectable IR band at 2120 cm^{-1} .^{11b} The cyanide bond lengths in **1** and **2** are 1.154(8)–1.157(8) Å and 1.142(5) Å, and the $\nu(\text{CN})$ bands were observed at 2113 and 2118 cm^{-1} , respectively.

Electrochemistry. The cyclic voltammograms (CV) of **1** and **2** are identical; that of **1** in CH_3CN (0.1 M (*n*-Bu₄N)PF₆) is shown in Figure 2. Two quasi-reversible two-electron-transfer processes are clearly observed at $E_{1/2}^1 = 0.01$ V and $E_{1/2}^2 = 0.96$ V (vs SSCE) with the peak separations, ΔE_p^1 and ΔE_p^2 , being 120 and 150 mV, respectively. The numbers of exchanged electrons for each redox wave were confirmed by controlled-potential coulometry. The redox waves at 0.01 and 0.96 V are

(12) Zhan, S.; Meng, Q.; You, X.; Wang, G.; Zheng, P. *Polyhedron* **1996**, *15*, 2655.

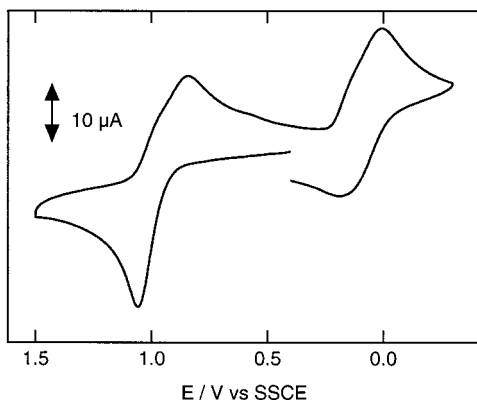
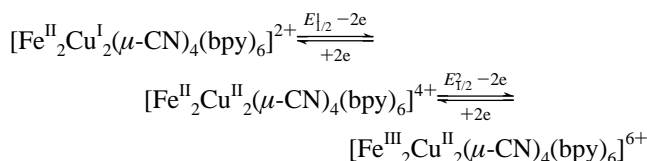


Figure 2. Cyclic voltammogram of **1** in acetonitrile. Conditions: 1 mM of **1**, 0.1 M (*n*-Bu₄N)PF₆, glassy carbon electrode, platinum wire counter electrode, SSCE reference, scan rate 100 mV s⁻¹.

respectively attributable to the Cu⁺/Cu²⁺ and Fe²⁺/Fe³⁺ process, which was depicted as follows:



It should be noted that electronic interactions between Fe^{•••}Fe and Cu^{•••}Cu ions through the {–CN–Cu–NC–} and {–NC–Fe–CN–} groups are rather small from the electrochemical viewpoints. The mononuclear complex, [Fe^{II}(CN)₂(bpy)₂], showed a reversible Fe^{II}/Fe^{III} redox wave at 0.47 V (vs SSCE), which is less positive than that of the same oxidation process for **1** (0.96 V). The more positive oxidation potential for **1** can be understood by two factors. (i) The molecular charge difference: It is expected that the complex with the higher molecular charge like **1** should show a higher oxidation potential. (ii) The lower electron density on the Fe²⁺ ion in **1**: In the molecular square, the [Cu^{II}(bpy)]²⁺ group may act as a Lewis acid, which leads to the higher oxidation potential for **1**.

Magnetic Properties. The temperature dependence of magnetic susceptibility for **1** and **2** was measured down to 2.0 K. In **1**, the Fe²⁺ ions are in the low-spin states (*S* = 0) and each Cu²⁺ ion has an unpaired electron (*S* = 1/2). The room temperature $\chi_m T$ value of **1** is 0.87 emu⁻¹ K mol⁻¹, which would be expected for an isolated two-spin system with a *g* value of 2.154, and $\chi_m T$ remains at a constant plateau down to 10 K. The magnetic data of **1** revealed that magnetic interactions between Cu²⁺ ions through the low-spin Fe²⁺ ions are negligibly small. The temperature dependence of the magnetic data for **2** is depicted in Figure 3. The molecular square of **2** consists of two of low-spin Fe³⁺ (*S* = 1/2) and Cu²⁺ (*S* = 1/2) ions. The $\chi_m T$ value of **2** at 300 K is 1.59 emu K mol⁻¹, which is characteristic of non-interacting four-spin systems of *S* = 1/2. As the temperature is lowered, the $\chi_m T$ value shows a gradual increase, reaching the maximum value (2.22 emu K mol⁻¹) at 7.0 K, and then a decrease. This observed temperature dependence of the $\chi_m T$ above 7 K is quite characteristic of ferromagnetically coupled systems. The magnetic data of **2** was analyzed by the four-spin model with exchange-coupling constants *J*₁ and

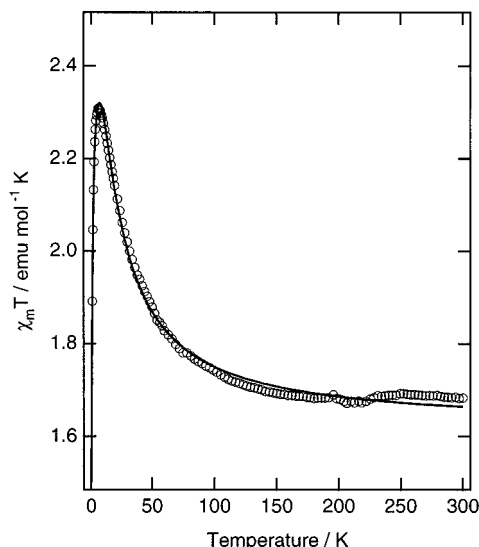


Figure 3. $\chi_m T$ vs *T* plot for **2**. The solid line corresponds to the theoretical curves, of which parameters are given in the text.

*J*₂ representing magnetic interactions between the adjacent Fe³⁺••Cu²⁺ ions and between the diagonal Fe³⁺•••Fe³⁺ and Cu²⁺•••Cu²⁺ ions, respectively, where the magnetic interactions through the cyanide ions and through the diagonal interactions were respectively treated as being identical. The energy eigenvalues were calculated by using the isotropic Heisenberg Hamiltonian of eq 1.

$$H = -2J_1(S_1 \cdot S_2 + S_2 \cdot S_3 + S_3 \cdot S_4 + S_4 \cdot S_1) - 2J_2(S_1 \cdot S_3 + S_2 \cdot S_4) \quad (1)$$

The resulting expression of $\chi_m T$ derived by Kambe's method¹³ is

$$\chi_m T = \frac{Ng^2\beta^2}{3k} \{30 \exp[(2J_1 + 4J_2)/kT] + 6 \exp[(-2J_1 + 4J_2)/kT] + 6 \exp(2J_2/kT) + 6 \exp[\exp(-2J_1 + 2J_2)/kT]\} / \{5 \exp[(2J_1 + 4J_2)/kT] + 3 \exp[(-2J_1 + 4J_2)/kT] + \exp[(-4J_1 + 4J_2)/kT] + 4 \exp(2J_2/kT) + 4 \exp[\exp(-2J_1 + 2J_2)/kT]\}$$

The least squares calculation yielded the best fitting parameters of *g*, *J*₁, and *J*₂ values being 2.077(1), and 6.3(1) cm⁻¹, and -3.1(1) cm⁻¹, respectively. In the molecular square of **2**, the Fe³⁺ and Cu²⁺ ions, each having *d*π and *d*σ spin, respectively, are alternately bridged by the cyanide ions and the strict orthogonality in the square leads to the quintet spin ground state.

Acknowledgment. This work was partially supported by a Grant-in-Aid for Scientific Research from the Ministry of Education, Science, Sports and Culture, Japan.

Supporting Information Available: X-ray crystallographic files in CIF format for **1** and **2**. This material is available free of charge via the Internet at <http://pubs.acs.org>.

IC990617L

(13) Kambe, K. *J. Phys. Soc. Jpn.* **1950**, *5*, 48.